Research Article | Vol. 31, No. 20 / 25 Sep 2023 / Optics Express 32900
Optics EXPRESS

Remote terahertz wireless power transfer with self-resonating spoof plasmonic structures

SHU-LING CHENG,[1] HONG-WEI WU,[1,2,3,*] WEN-JUN SUN,[1] NONG ZHOU,[1] CHENG-YAO PENG,[2,4] ZONG-QIANG SHENG,[1] AND WEN-BING ZHANG[2]

[1]School of Mechanics and Photoelectric Physics, Anhui University of Science and Technology, Huainan 232001, China
[2]Institute of Energy, Hefei Comprehensive National Science Center (Anhui Energy Laboratory), Hefei 230031, China
[3]National Laboratory of Solid State Microstructures, Nanjing University, Nanjing 210093, China
[4]pengcy@ie.ah.cn
[*]hwwu@aust.edu.cn

Abstract: In this paper, we use a pair of self-resonating subwavelength spoof plasmonic structures to achieve remote non-radiative terahertz wireless power transfer, while nearly without affecting the electromagnetic environment of free space around the structure. The resonating frequency and quality factor of the magnetic dipole mode supported by the spoof plasmonic structures can be freely tuned by tailoring the geometric structure. By putting the weak source and detector into the self-resonating structures, we can find that the effective non-radiative terahertz power transferring distance can reach several hundred times the radius of the structures. Finally, we also demonstrate the efficient wireless power transfer capability for the multi-target receiving system. These results may provide a novel approach to the design of non-radiative terahertz wireless power transfer and communications.

1. Introduction

Wireless power transfer (WPT) is a kind of noncontact power transmission system, which is experimentally investigated by Nikola Tesla in the early 20th century [1]. The approach of power transfer provides an ideal solution for most critical electronic devices installed in hard-to-reach places, such as artificial cardiac pacemaker, biosensor and so on. Since the concept of the WPT was proposed, different WPT systems have been widely explored and demonstrated [2–9]. According to the transferring mechanism, the WPT can be divided into two categories, one is radiative WPT [10] and the other is non-radiative WPT [11]. Comparing to radiative WPT, the non-radiative WPT based on near-field coupling is more proper for most daily devices by considering power transfer efficiency and the safety issue. In 2007 years, an improved inductive power transfer system is proposed to achieve high efficiency and long transmission distance based on magnetic resonance coupling between the transmitter and the receiver [12]. Based on the near-field coupling, the quality factor (Q-factor) of self-resonating structures and coupling coefficient between the structures play important roles in the WPT performance. For increasing the Q-factor, various novel resonators have been designed, such as metallic-coil based resonators [13–15], dielectric resonators [16,17], and cavity mode resonators [18,19]. For enhancing the coupling efficiency and controlling the power transfer route, the metamaterials and metasurfaces also been introduced to tailor the near-field and manipulate the coupling between the transmitter and the receiver ends [20–23]. Terahertz (THz) wave, as information carrier of new generation communication, recently has been widely investigated, and various THz functional devices have been designed to manipulate THz wave for communication, sensing and bio-imaging. Thus, terahertz WPT also has vital significance for these THz functional devices.

#492279 https://doi.org/10.1364/OE.492279
Journal © 2023 Received 3 Apr 2023; revised 11 Jul 2023; accepted 8 Sep 2023; published 19 Sep 2023

Optics EXPRESS

In THz wave range, the concept of spoof localized surface plasmons (LSPs) has been proposed based on the textured perfect electric conductor (PEC) cylinder for simulating the LSPs in optical band supporting on metallic nanoparticles [24]. Particularly, the three-dimensional spoof localized surface plasmonic structure is found that not only supports electric spoof LSPs, but also supports magnetic spoof LSPs at deep subwavelength scale [25]. However, the maximum magnetic field of magnetic LSPs is confined inside the whole structure and hard to focus the field. To avoid the disadvantage, we recently design and demonstrate that a hollow spoof surface plasmonic structure can supports electric and magnetic multipole resonances in two-dimensional and three-dimensional structure similar to the Mie-resonances in all-dielectric particles [26–28], simultaneously. The hollow structures can focus the magnetic field in the center of structure and interact with the magnetic dipole to enhance emission [29]. Comparing with all-dielectric structure with high index, the spoof surface plasmonic structure has a greater freedom degree for tuning resonant strength and frequency by tailoring the geometry parameters. To have high Q-factor, we also design spiral structure to increase the Q-factor by increasing the spiral degree [30]. The tunable hollow spoof surface plasmonic structure, which can focus the magnetic resonance in structure center interacted with the transmitter and receiver, may provide a versatile platform to achieve THz wireless power transfer.

In this paper, we design a pair of self-resonating hollow spoof plasmonic structures to achieve remote non-radiative THz wireless power transfer. We numerically demonstrate that spoof plasmonic structure not only support magnetic dipole mode with high Q-factor, but also can freely tuning the resonating frequency of magnetic mode by changing the structure parameters. Based on these the advantages, we investigate the THz wireless power transfer by putting a pair of the magnetic dipole source and detector into the center of two self-resonating spoof plasmonic structures, and find that the power of the THz source is efficiently transferred to the receiver end crossed a long distance comparing with a pair bare THz source and detector. Simultaneously, it is nearly without affecting the electromagnetic environment of free space. Moreover, we also show that the efficient WPT capability can be achieved from one source to the multi-target receiving system. These results maybe provide a novel approach to design the non-radiative terahertz wireless power transfer and communications.

2. Results and discussion

By periodically inserting the metallic strips made with perfect electrical conductor (PEC) as the yellow part into the hollow silicon cylinder as the green region, a subwavelength spoof plasmonic structure with outer radius of R and inner radius of r is formed, as shown as Fig. 1(a). The length and width of PEC strip are denoted as R - r and a, and the number of PEC strips are N, thus the period of subwavelength structure can be expressed as $d = 2\pi R/N$. Based on the finite element analysis with the commercial software COMSOL Multiphysics, we simulate the electromagnetic response and field distribution of two-dimensional (2D) structures by considering the excitation of incident plane waves with transverse magnetic field (H_z) polarization, and use the scattering cross section (SCS) normalized to $2R$ to represent the electromagnetic response of hollow structures with negligible absorption. Without loss of generality, we choose the structure parameters as follows: the number of PEC strips $N = 30$, the width of PEC strips $a = 8.373$μm, outer radius $R = 50$μm, inner radius $r = 10$μm, and the ratio a / $d = 0.8$ in the azimuthal direction. As shown in Fig. 1(b), we can find that the normalized SCS presents a magnetic dipole (MD) resonating peak at 0.514THz. In order to further verify the origin of the resonating peak, the near field distribution $|H_{sca}|$ of structure at resonating frequency $f = 0.514$THz is given in inset of Fig. 1(b). It is not difficult to find that the mode distribution of the magnetic field appears as a circular spot pattern and the maximum magnetic field intensity is located in the hollow of the structure corresponding to magnetic dipole resonating mode.

Optics EXPRESS

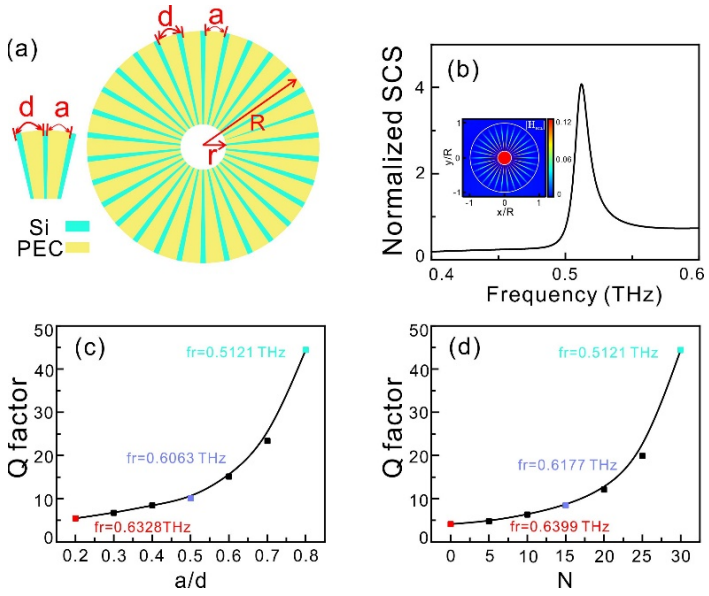

Fig. 1. (a) Schematic of subwavelength hollow spoof plasmonic structure. (b) Normalized SCS and near field distribution of the MD mode. (c) The relationship between Q factor of the MD mode and a/d. The points with f_r = 0.6328, 0.6063, 0.5121THz corresponding to the resonating frequencies of the MD modes for the ratio a / d = 0.2, 0.5, 0.8. (d) The influence of changing the number of metal strips N on Q factor. The resonating frequency f_r = 0.6399, 0.6177, 0.5121THz corresponding to the MD modes for metallic strip number as 0, 15, 30.

To obtain high-Q factor of the MD mode for realizing efficient terahertz WPT, we firstly investigated the influence of the ratio a / d on the Q factor of MD mode in Fig. 1(c). The results show that the Q factor will increases with the increase of the ratio a / d, which indicates that the structure has stronger field confined capability. While the resonating frequency of the MD mode also vary with changing the ratio a / d. We denote the resonating frequency f_r = 0.6328, 0.6063, 0.5121THz by red, dark blue and cyan points corresponding to the ratio a / d = 0.2, 0.5, 0.8 in Fig. 1(c). We can find that the resonating frequency will decrease with increasing the ratio. Similarly, we also calculate the Q-factor and resonating frequency of the MD modes varying with changing metallic strip number N in Fig. 1(d). Obviously, with the increase of the number of PEC strips N, the Q-factor increases and the resonance frequency decreases. In fact, for practical metallic strips (such as gold, silver and copper) in THz frequency regime, the material absorption loss is obvious for increasing the metallic parts (increasing a / d and strip number N), thus the Q factors in Figs. 1(c) and (d) will have a maximum value as discussed in our previous work [31]. Here, we main focus the Q factor varying with the structure parameters, the practical metal will be discussed in Fig. 4. It is well known that the larger the Q factor is, the stronger the non-radiative characteristics of the structure will be. Thus, the spoof plasmonic structures supported MD modes with high Q factor provide a versatile platform to realize remote non-radiative terahertz WPTs.

Next, we will use two spoof plasmonic structures with the same parameters which support the strong magnetic dipole resonance to realize the remote non-radiative terahertz WPT system, as shown in Fig. 2(a). The distance between the two subwavelength structures is L. The transmitter (denoted by "T") is excited by an internal weak MD source represented by a purple solid dot; the red solid dot is used to detect the magnetic field at the receiver (denoted by subscript "D").

Optics EXPRESS

For the terahertz MD emitter, it can be fabricated in the materials which have the strong MD transitions (such as $TmFeO_3$ and $ErFeO_3$) by filling the structural hollow as quantum dots in the specific solution [32]. The distance between the transmitter ("T") and the receiver ("D") is $L = 32R = 1600\mu m$. We conduct full-wave simulations for the MD source excitation in the 2D scenario based on finite element analysis with COMSOL Multiphysics. To verify the system's remote terahertz WPT capability, we firstly detect the magnetic field intensity $|H_0|$ for direct transfer from source to detector in free space shown in left panel of Fig. 2(b). As shown in left panel of Figs. 2(c)-(e), we calculated the enhancement of magnetic field detected at the receiver $|H_D|/|H_0|$, $|H_T|/|H_0|$ and $|H_{TD}|/|H_0|$ transferred for three cases: placing the structure only at the receiver as Fig. 2(c), placing the structure only at the transmitter as Fig. 2(d), and placing the structure both at the transmitter and the receiver as Fig. 2(e). It is clearly observed that the enhancement magnetic field $|H_D|/|H_0|$ and $|H_T|/|H_0|$ at the MD resonance frequency of 0.511THz can be nearly up to a factor of 50 when the designed structure is placed only at the receiver or transmitter. More importantly, in our design of the transfer system consisting of the same subwavelength structures simultaneously placed at both the transmitter and the receiver, the enhancement magnetic field $|H_{TD}|/|H_0|$ can reach nearly 2500. The right panel in Figs. 2(b)-(e) shows the magnetic field distributions at the MD resonance frequency of 0.511THz. By comparison, we can see that the detected magnetic field at the receiver is significantly enhanced for using the spoof plasmonic structures, while keeping the magnetic field intensity along the transfer path much lower than the receiver. In the near-field region, when $L < 12R$, we find that the magnetic field intensity with the structure placed at both the transmitter and the receiver is greater than the product of the magnetic field intensity with the structure placed at only one end $|H_{TD}||H_0| > |H_T||H_D|$, the reason is that the strong MD-MD interaction between the two resonators. For the far-field region, when $L > 12R$, the transfer process can be divided into two cascaded processes: transmitting and receiving power, which can be regarded as $|H_{TD}||H_0| \approx |H_T||H_D|$. Here, the near field extends by less than one wavelength. The far field occurs where the distance from the dipole is much greater than one wavelength. Thus, we define the near field region when the distance L between two structures is less than twelve times the outer radius R, and similarly, the far field region for the distance L between two structures is greater than twelve times the outer radius R.

Furthermore, we study the effect of changing the parameters of the structure on the magnetic field enhancement factor $|H_{TD}|/|H_0|$ of the terahertz wireless power transfer system. As shown in Fig. 3(a), we study the influence of ratio a / d on the magnetic field enhancement $|H_{TD}|/|H_0|$. It is obvious that the magnetic field enhancement $|H_{TD}|/|H_0|$ increases with the increase of ratio a / d, and the resonant frequency is red-shifted. Furthermore, the half-peak width corresponding to the MD mode decreases with the increase of a / d, i.e., the Q factor of the MD mode increase as discussion as Fig. 1(c). It indicates that the structure with large a / d has stronger capability of confined field to achieve a non-radiative effect. In Fig. 3(b), we vary the outer radius R of the subwavelength structure from 35μm to 65μm, and keep others parameters as: the number of PEC strips $N = 30$, the width of PEC strips $a = 8.373\mu m$, inner radius $r = 10\mu m$, and the ratio a / $d = 0.8$, the distance between the transmitter ("T") and the receiver ("D") is $L = 32R = 1600\mu m$. We can observe that the magnetic field enhancement $|H_{TD}|/|H_0|$ increases first and then slightly decreases with the increase of the outer radius R, and the resonance frequency red-shifts with the increase of the outer radius R. Similarly, we vary the inner radius r of the subwavelength structure from 4μm to 16μm and keep the other parameters constant in Fig. 3(c). It can be seen from the results that the magnetic field enhancement $|H_{TD}|/|H_0|$ also shows a trend of first increasing and then decreasing with the increase of the inner radius r, and the resonance frequency also is red shifted with the increase of the inner radius r. Moreover, we investigate the variation of the magnetic field enhancement efficiency $|H_{TD}|/|H_0|$ when changing the transfer distance L from $10R$ to $400R$ in Fig. 3(d). It is intuitively found that the magnetic field enhancement

Optics EXPRESS

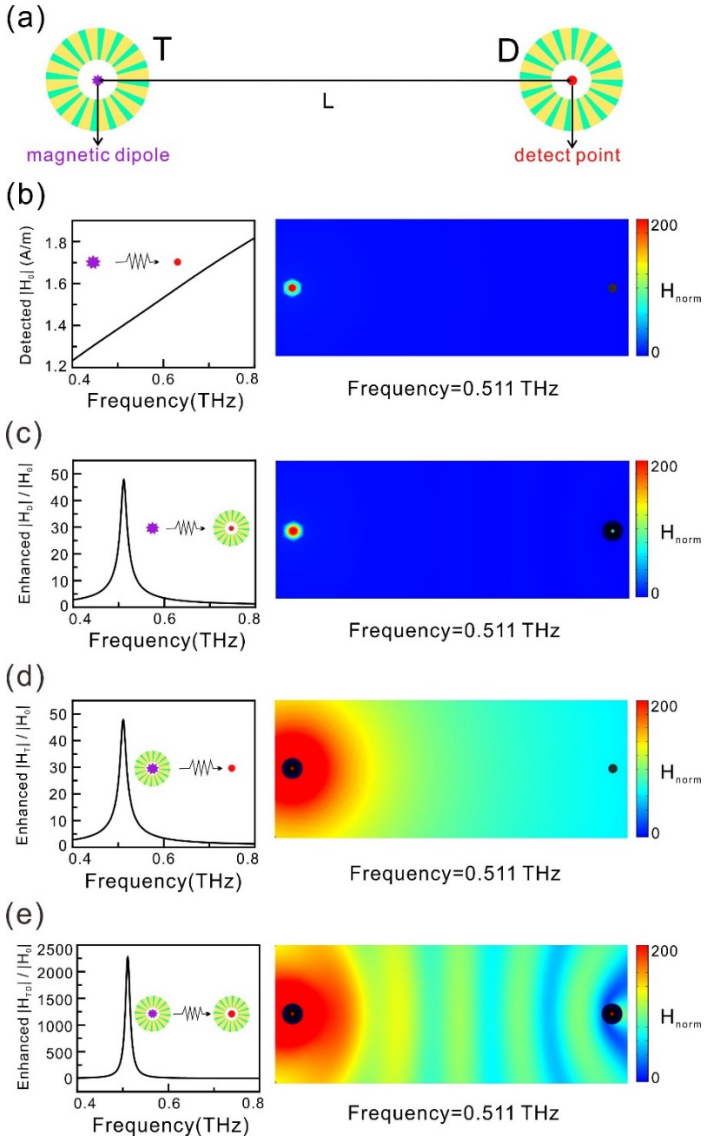

Fig. 2. (a) The schematic of remote non-radiative terahertz WPT system. "T" and "D" represent the resonators of transmitter and receiver. The purple solid dot in the center of the transmitter indicates the magnetic dipole source used for excitation, and the red solid dot is used to detect the magnetic field at the receiver. The left panel of (b) is the detected magnetic field intensity $|H_0|$ without structure placed in transmitter or receiver. The left panel of (c)-(e) are the magnetic field enhancement for three cases: the structure placed in receiver, the structure placed in transmitter and the structure placed in both transmitter and receiver. The insert of left panel is the schematic of three transfer system. The right panel of (b)-(e) are the magnetic field distribution at resonant frequency of 0.511THz.

Optics EXPRESS

efficiency $|H_{TD}|/|H_0|$ oscillates near the near-field when $L < 12R$ due to the strong MD-MD resonance interaction between the transmitter and receiver, and tends to be stable in the far-field when $L > 12R$. When the transmitter and receiver are placed close together, the spectrum of the transmitter overlaps with that of the receiver, which is analogous to the short-range dipole-dipole interaction between fluorescent emitters, i.e., Förster resonant energy transfer [33].

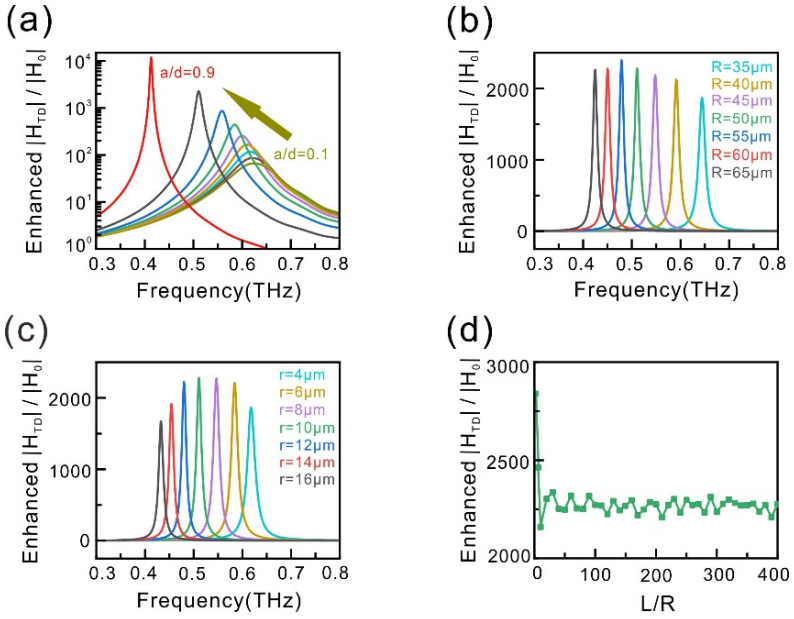

Fig. 3. (a)-(c) The influence of structural parameters on magnetic field enhancement $|H_{TD}|/|H_0|$ for different the outer radius R, different the inner radius r and different the ratio a / d. (d) The variation of the magnetic field enhancement efficiency $|H_{TD}|/|H_0|$ when changing the transfer distance L.

Next, we investigate the terahertz wireless power transfer in three-dimensional (3D) case. As shown in the inset of the Fig. 4(a), we consider a pair of finite-height subwavelength 3D structures with the height $h = 50\mu m$, the number of PEC strips $N = 30$, the width of PEC strips $a = 8.373\mu m$, outer radius $R = 50\mu m$, inner radius $r = 10\mu m$, the ratio $a / d = 0.8$, and the distance between the two subwavelength structures $L = 32R = 1600\mu m$ as the transmitter and receiver of the transfer systems. Surprisingly, we found that the magnetic field enhancement $|H_{TD}|/|H_0|$ in the 3D case can reach nearly four orders of magnitude. Then, we plot the magnetic field intensity $|H|$ along the center line from the transmitter to the receiver to demonstrate the non-radiative properties of the system in the Fig. 4(b). The solid purple line represents the detected magnetic field intensity $|H|$ with the magnetic dipole moment of the source $\boldsymbol{M} = 1 \times 10^{-10}$ m^2/A in the center of transmitter; solid red and green lines represent the magnetic field intensity $|H|$ detected in free space with the magnetic dipole moment $\boldsymbol{M} = 9 \times 10^{-7}$ m^2/A, 1×10^{-10} m^2/A of the source, respectively. By comparison, the system composed of the subwavelength structure designed shows obvious enhancement of the magnetic field intensity at the receiver and reduction of the magnetic leakage around the structure. The magnetic field distribution of terahertz WPT system is shown in the inset in Fig. 4(b), which further demonstrates that the system has the remote non-radiative transfer capability. In addition, the effect of the height h variation of the 3D structure on the magnetic field enhancement is studied shown in Fig. 4(c). The results show that the magnetic field enhancement $|H_{TD}|/|H_0|$ first increases with the increase of height h from 20μm to 80μm, and the frequency of the MD resonance is red shifted. In the above investigations,

Optics EXPRESS

the metallic material is usually assumed as the PEC in our designed structure. In Fig. 4(d), we calculate the magnetic field enhancement $|H_{TD}|/|H_0|$ when the PEC is replaced by the actual metal, the black line represents Ag, the red line represents Cu, and the blue line represents Al. Due to the inherent Ohmic loss of the metal, the magnetic field enhancement is reduced, but it can still reach nearly three orders of magnitude enhancement at the lowest in resonance frequency.

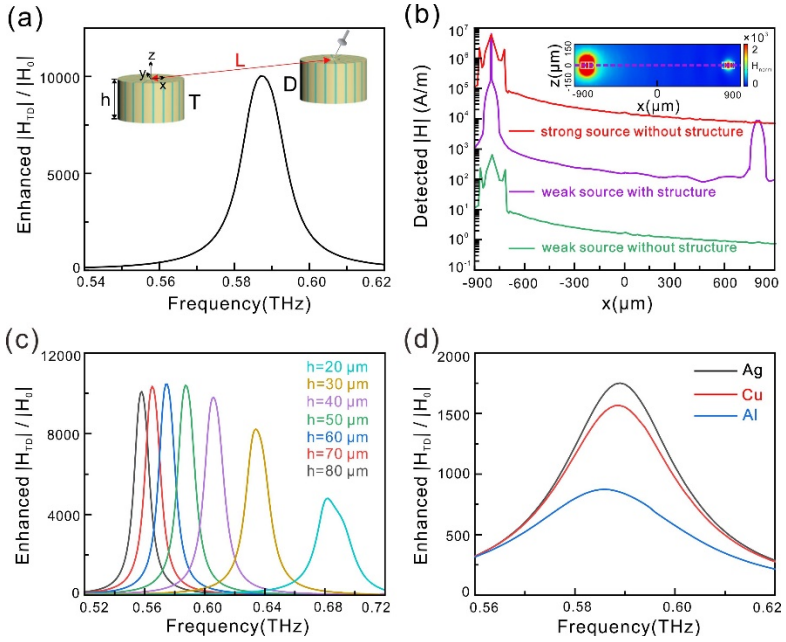

Fig. 4. (a) Magnetic field enhancement $|H_{TD}|/|H_0|$ in 3-D case. T and D represent the resonator at the transmitter and the resonator at the receiver, respectively. The insert of (a) is the transfer system in 3-D case. (b) The magnetic field intensity $|H|$ along the center line for y = 0 and z = 0 from the transmitter to the receiver in 3 case: a strong MD source $\boldsymbol{M} = 9 \times 10^{-7}$ m^2/A placed in free space (shown by solid red line), a weak MD source $\boldsymbol{M} = 1 \times 10^{-10}$ m^2/A placed in the center of transmitter (shown by solid purple line), a weak MD source $\boldsymbol{M} = 1 \times 10^{-10}$ m^2/A placed in free space (shown by solid green line). The inset of (b) is the magnetic field distribution correspond to the solid purple line. (c) The magnetic field enhancement $|H_{TD}|/|H_0|$ varies with height h from 20μm to 80μm. (d) The magnetic field enhancement $|H_{TD}|/|H_0|$ for three actual metal.

Finally, we investigate the remote non-radiative terahertz WPT system with multiple receivers (marked by "D1", "D2" and "D3"). As shown in the inset of the Fig. 5(a), the structural parameters of the transmitter and receiver are as follows: the height $h = 50$μm, outer radius $R = 50$μm, inner radius $r = 10$μm, the number of PEC strips $N = 30$, the width of PEC strips $a = 8.373$μm, the ratio $a / d = 0.8$, and the distance between the transmitter and receiver is $L1 = 1600$μm, $L2 = 824.62$μm, $L3 = 916.51$μm, respectively. We place a MD source inside the center of the transmitter for excitation, and the magnetic field enhancement $|H_{TD}|/|H_0|$ detected inside the three receivers is shown in Fig. 5(a). The magnetic field enhancement $|H_{TD}|/|H_0|$ detected at all three receivers can reach nearly 10^4. Figure 5(b) shows the magnetic field distribution obtained at the magnetic dipole resonance position, and the coordinates of the three receivers are given in red letters. We can clearly see that the magnetic field at the three receivers is enhanced and much higher than the surrounding environment. Therefore, the system designed by us can realize the multi-target remote non-radiative terahertz wireless power transfer.

Optics EXPRESS

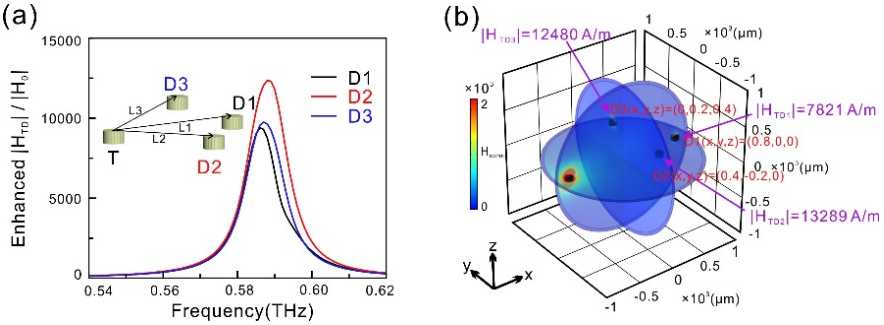

Fig. 5. (a) Magnetic field enhancement $|H_{TD}|/|H_0|$ corresponding to the three receivers. The insert of (a) is the schematic diagram of multi-target remote non-radiative terahertz wireless power transfer system. The distance between transmitter and receiver are $L1 = 1600\mu m$, $L2 = 824.62\mu m$, $L3 = 916.51\mu m$. (b) The magnetic field distribution at magnetic dipole resonance frequencies. The coordinates of three detector are D1(x, y, z) = (0.8, 0, 0), D2(x, y, z) = (0.4, -0.2, 0), D3(x, y, z) = (0, 0.2, 0.4). The coordinate of transmitter is T(x, y, z) = (-0.8, 0, 0).

3. Conclusion

In summary, we have presented a system formed by a pair of subwavelength spoof plasmonic structures for remote non-radiative terahertz wireless power transfer. The results show that the effective non-radiative terahertz wireless power transfer distance is several hundred times the radius of the structure, and the surrounding electromagnetic environment is basically unaffected. In addition, we also investigate the effect of geometric parameters of self-resonant artificial plasmonic structures on resonance frequency and transfer efficiency, which provides a great degree of freedom for structure design. Finally, we also verify the high efficiency wireless power transfer capability of the multi-target transfer system in the three-dimensional case. Our work may provide a new way for the design of wireless power transfer devices and communication devices.

Funding. University Synergy Innovation Program of Anhui Province (GXXT-2022-015); Major Scientific Research Projects of Colleges and Universities in Anhui Province (2022AH040114).

Acknowledgments. The authors acknowledge support from the Major Scientific Research Projects of Colleges and Universities in Anhui Province (Grant No. 2022AH040114); the University Synergy Innovation Program of Anhui Province (Grant No. GXXT-2022-015).

Disclosures. The authors declare no conflicts of interest

Data availability. Data underlying the results presented in this paper are not publicly available at this time but may be obtained from the authors upon reasonable request.

References

1. N. Tesla, "Apparatus for transmitting electrical energy," U.S. Patent **1**(119), 732 (1914).
2. A. Karalis, J. D. Joannopoulos, and M. Soljacic, "Efficient wireless non-radiative mid-range energy transfer," Ann. Phys. **323**(1), 34–48 (2008).
3. M. Song, I. Iorsh, P. Kapitanova, E. Nenasheva, and P. Belov, "Wireless power transfer based on magnetic quadrupole coupling in dielectric resonators," Appl. Phys. Lett. **108**(2), 023902 (2016).
4. X. Shi, C. Qi, M. Qu, S. Ye, G. Wang, L. Sun, and Z. Yu, "Effects of coil shapes on wireless power transfer via magnetic resonance coupling," Electromagn. Waves Appl. **28**(11), 1316–1324 (2014).
5. M. Falavarjani and M. Shahabadi, "Design and implementation of compact WPT system using printed spiral resonators," Electron. Lett. **50**, 110–111 (2014).
6. B. Tierney and A. Grbic, "Design of self-matched planar loop resonators for wireless nonradiative power transfer," IEEE Trans. Microwave Theory Techn. **62**(4), 909–919 (2014).
7. M. J. Chabalko and A. P. Sample, "Resonant cavity mode enabled wireless power transfer," Appl. Phys. Lett. **105**(24), 243902 (2014).

Optics EXPRESS

8. W. Wang, S. Hemour, and K. Wu, "Coupled resonance energy transfer over gigahertz frequency range using ceramic filled cavity for medical implanted sensors," IEEE Trans. Microwave Theory Techn. **62**(4), 956–964 (2014).
9. Y. Xie, Z. Zhang, Y. Lin, T. Feng, and Y. Xu, "Magnetic quasi-bound state in the continuum for wireless power transfer," Phys. Rev. Appl. **15**(4), 044024 (2021).
10. W. C. Brown, "The technology and application of free-space power transmission by microwave beam," Proc. IEEE **62**(1), 11–25 (1974).
11. L. Ka-Lai, J. W. Hay, and P. G. W. Beart, "Contact-less power transfer," *U.S. patent* 7042, 196 (2006).
12. A. Kurs, A. Karalis, R. Moffatt, J. D. Joannopoulos, P. Fisher, and M. Soljacich, "Wireless power transfer via strongly coupled magnetic resonances," Science **317**(5834), 83–86 (2007).
13. E. M. Thomas and J. D. Heebl, "A power link study of wireless non-radiative power transfer systems using resonant shielded loops," IEEE Trans. Circuits Syst. I **59**(9), 2125–2136 (2012).
14. B. B. Tierney and A. Grbic, "Planar shielded-loop resonators," IEEE Trans. Antennas Propagat. **62**(6), 3310–3320 (2014).
15. S. R. Khan and G. Choi, "Analysis and optimization of four-coil planar magnetically coupled printed spiral resonators," Sensors **16**(8), 1219 (2016).
16. M. Song, P. Kapitanova, and P. Belov, "Wireless power transfer based on dielectric resonators with colossal permittivity," Appl. Phys. Lett. **109**(22), 223902 (2016).
17. M. Song, P. Belov, and P. Kapitanova, "High permittivity dielectric resonators for wireless power transfer system," *International Symposium on Antennas and Propagation* 153–154 (iEEE, 2016).
18. M. J. Chabalko and A. P. Sample, "Three-dimensional charging via multimode resonant cavity enabled wireless power transfer," IEEE Trans. Power Electron. **30**(11), 6163–6173 (2015).
19. M. J. Chabalko, M. Shahmohammadi, and A. P. Sample, "Quasistatic cavity resonance for ubiquitous wireless power transfer," PLoS One **12**(2), e0169045 (2017).
20. Y. Urzhumov and D. R. Smith, "Metamaterial-enhanced coupling between magnetic dipoles for efficient wireless power transfer," Phys. Rev. B **83**(20), 205114 (2011).
21. B. Wang, K. H. Teo, T. Nishino, W. Yerazunis, J. Barnwell, and J. Zhang, "Experiments on wireless power transfer with metamaterials," Appl. Phys. Lett. **98**(25), 3601927 (2011).
22. L. Zhu, X. Luo, and H. Ma, "Distant and wide range wireless power transfer from metamedia," Appl. Phys. Lett. **109**(2), 024103 (2016).
23. W. C. Harris, D. D. Stancil, and D. S. Ricketts, "Improved wireless power transfer efficiency with non-perfect lenses," Appl. Phys. Lett. **114**(14), 143903 (2019).
24. A. Pors, E. Moreno, L. Martin-Moreno, J. B. Pendry, and F. J. Garcia-Vidal, "Localized spoof plasmons arise while texturing closed surfaces," Phys. Rev. Lett. **108**(22), 223905 (2012).
25. P. A. Huidobro, X. Shen, J. Cuerda, E. Moreno, L. Martin-Moreno, F. J. Garcia-Vidal, T. J. Cui, and J. B. Pendry, "Magnetic Localized Surface Plasmons," Phys. Rev. X **4**(2), 021003 (2014).
26. H. W. Wu, Y. Z. Han, H. J. Chen, Y. Zhou, X. C. Li, J. Gao, and Z. Q. Sheng, "Physical mechanism of order between electric and magnetic dipoles in spoof plasmonic structures," Opt. Lett. **42**(21), 4521 (2017).
27. H. W. Wu, Y. Li, H. J. Chen, Z. Q. Sheng, H. Jing, R. H. Fan, and R. W. Peng, "Strong Purcell effect for terahertz magnetic dipole emission with spoof plasmonic structure," ACS Appl. Nano Mater. **2**(2), 1045–1052 (2019).
28. S. L. Cheng, H. W. Wu, and Y. Q. Yin, "Ultrastrong Purcell enhancement of magnetic dipole emission based on quasi-BIC," Eur. Phys. J. D **76**(11), 211 (2022).
29. H. W. Wu, H. J. Chen, H. F. Xu, R. H. Fan, and Y. Li, "Tunable multiband directional electromagnetic scattering from spoof Mie resonant structure," Sci. Rep. **8**(1), 8817 (2018).
30. H. W. Wu, J. Q. Quan, Y. Q. Yin, and Z. Q. Sheng, "Strong Purcell effect for magnetic dipole emission with spoof plasmonic spiral structure," J. Opt. Soc. Am. B **37**(1), 98 (2020).
31. H. W. Wu, Y. Fang, J. Q. Quan, Y. Z. Han, Y. Q. Yin, Y. Li, and Z. Q. Sheng, "Multifrequency superscattering with high Q factors from a deep-subwavelength spoof plasmonic structure," Phys. Rev. B **100**(23), 235443 (2019).
32. R. Mikhaylovskiy, T. J. Huisman, R. V. Pisarev, T. Rasing, and A. V. Kimel, "Selective Excitation of Terahertz Magnetic and Electric Dipoles in Er3+ Ions by Femtosecond Laser Pulses in ErFeO3," Phys. Rev. Lett. **118**(1), 017205 (2017).
33. T. Förster, "Zwischenmolekulare energiewanderung und fluoreszenz," Ann. Phys. **437**(1-2), 55–75 (1948).